18. W. Dansgaard *et al.*, *Nature* **364**, 218 (1993); S. J. Johnsen *et al.*, *Nature* **359**, 311 (1992).

19. K. G. Cannariato and J. P. Kennett, *Geology* **27**, 975 (1999); K. G. Cannariato, J. P. Kennett, R. J. Behl, *Geology* **27**, 63 (1999).

20. I. L. Hendy and J. P. Kennett, in preparation.

21. A. Van Geen *et al.*, *Paleoceanography* **11**, 519 (1996).

22. Samples (2 cm thick, averaging 14 years) were taken every 5 to 7 cm (50 to 70 years). Sampling resolution is lower between 13 and 25 ka. From 8 to 40 planktonic and 5 to 10 benthic foraminifera were picked from each sample for analysis using a Finnigan/MAT 251 light stable isotope mass spectrometer and standard preparation techniques. Instrumental precision is <0.09‰ for both isotopes, with all data expressed as standard δ notation in ‰ relative to the Pee Dee Belemnite, related by repeated analysis to NBS-19 and NBS-20. The chronology is based on 17 accelerator mass spectrometry radiocarbon dates and three SPECMAP datums (*15–17*), as the ODP Hole 893A benthic foraminiferal δ18O record correlates well with the standard late Quaternary δ18O stratigraphy.

23. J. P. Kennett *et al.*, Eds., *Proc. Ocean Drill. Program Initial Reports* **146** (part 2) (Ocean Drilling Program, College Station, TX, 1994); J. P. Kennett *et al.*, Eds., *Proc. Ocean Drill. Program Sci. Results* **146** (part 2) (Ocean Drilling Program, College Station, TX, 1994).

24. Properties of kerogen in Hole 893A suggest an episodic recycling of CH_4 in basin sediments [L. M. Pratt, A. M. Carmo, V. Brüchert, S. M. Monk, J. M. Hayes, in J. P. Kennett *et al.*, Eds., *Proc. Ocean Drill. Program Sci. Results* **146** (part 2) (Ocean Drilling Program, College Station, TX, 1994), pp. 213–218].

25. J. W. Yun, D. L. Orange, M. E. Field, *Mar. Geol.* **154**, 357 (1999).

26. J. P. Kennett and C. C. Sorlien, *AAPG Bull.* **83**, 692 (1998).

27. I. L. Hendy and J. P. Kennett, *Paleoceanography* **15**, 30 (2000).

28. The benthic δ13C record is based on several species since no benthic species ranges throughout the sequence because of extreme changes in basin oxygenation associated with D-O cycles. Overlap of a few species allows interspecies δ13C stadial-interstadial comparisons. For interstadials, we analyzed *Bolivina argentea*, *Bolivina tumida*, *Buliminella tenuata*, and *Bolivina spissa*; for stadials, we analyzed *Uvigerina peregrina* and *Rutherfordoides rotundata*. For short key intervals, we also analyzed *Globobulimina auriculata*, *Buliminella subfusiformis*, and *Bolivina advena*. We produced complete δ13C records of *Globigerina bulloides* (surface water) and *Neogloboquadrina pachyderma* (thermocline) [D. Pak, J. P. Kennett, M. Kashgarian, *Eos* **78**, 359 (1997)] and short records of *Globigerina quinqueloba* (surface water) and *Globorotalia scitula* (subthermocline) [J. D. Ortiz, A. C. Mix, R. W. Collier, *Paleoceanography* **10**, 987 (1995); J. D. Ortiz *et al.*, *Geochim. Cosmochim. Acta* **60**, 4509 (1996)].

29. J. P. Kennett and M. S. Srinivasan, *Neogene Planktonic Foraminifera: A Phylogenetic Atlas* (Hutchinson Ross, Stroudsburg, PA, 1983).

30. Overlapping taxonomic ranges between stadials and interstadials at some levels are reflected only by rare specimens that may be environmentally unrepresentative of that climatic episode.

31. W. H. Berger and E. Vincent, *Geol. Rundsch.* **75**, 249 (1986).

32. D. C. McCorkle and S. R. Emerson, *Geochim. Cosmochim. Acta* **52**, 1169 (1988); D. C. McCorkle and G. P. Klinkhammer, *Geochim. Cosmochim. Acta* **55**, 161 (1991); J. M. Bernhard, B. K. Sen Gupta, P. F. Borne, *J. Foram. Res.* **27**, 301 (1997).

33. R. Zahn, K. Winn, M. Sarnthein, *Paleoceanography* **1**, 27 (1986); D. C. McCorkle *et al.*, *Paleoceanography* **5**, 161 (1990); G. J. Van der Zwaan *et al.*, *Earth Sci. Rev.* **46**, 213 (1999).

34. G. Wefer, P. M. Heinze, W. H. Berger, *Nature* **369**, 282 (1994).

35. Within the ocean, oxidation of CH_4 to CO_2 is carried out by methanotrophic bacteria (*5*), which decreases DIC δ13C values. Bicarbonate ion incorporation during shell growth transfers the negative δ13C value to foraminiferal $CaCO_3$. Negative δ13C values may also be taken up by foraminifera through consumption of methanotrophic bacteria.

36. J. P. Kennett, unpublished data.

37. R. O. Barnes and E. E. Goldberg, *Geology* **4**, 297 (1976); A. L. Warford, D. R. Kosiur, P. R. Doose, *Geomicrobiol. J.* **1**, 117 (1979).

38. W. S. Borowski, C. K. Paull, W. Ussler III, *Geology* **24**, 655 (1996).

39. F. J. Cynar and A. A. Yayanos, *J. Geophys. Res.* **97**, 11269 (1992).

40. V. Gornitz and I. Fung, *Global Biogeochem. Cycles* **8**, 335 (1994).

41. Y. Zhang, personal communication.

42. J. Chappell *et al.*, *Earth Planet. Sci. Lett.* **141**, 227 (1996).

43. The amount of CH_4 responsible for changing the δ13C of DIC of entire water column (~500 m) by ~3‰ (the average foraminiferal isotopic change during the 44.1-ka excursion) can be calculated from this relationship: $\delta^{13}C_{CH4}(C_{CH4}) + \delta^{13}C_{DIC\ before}(C_{DIC\ before}) = \delta^{13}C_{DIC\ after}(C_{DIC\ after})$. The calculation for instantaneous carbon transfer assumes basin volume of 850 km³; methane δ13C of −65‰; and DIC of 2000 µmol/kg. The time-dependent calculation assumes an event duration of 14 years; residence time of surface waters in Santa Barbara Channel of 30 days. We infer a longer residence time compared with the present day (~10 days) [M. C. Henderscott, *Fifth California Islands Symposium*, 29 March to 1 April 1999, Santa Barbara, p. 21; S. Harms and C. D. Winant, *J. Geophys. Res.* **103**, 3041 (1998)] because

44. M. A. K. Khalil and R. A. Rasmussen, in *Composition, Chemistry, and Climate of the Atmosphere*, H. B. Singh, Ed. (Van Nostrand Reinhold, New York, 1995), pp. 50–87.

45. R. Stauffer *et al.*, *Nature* **392**, 59 (1998).

46. E. G. Nisbet, *Can. J. Earth Sci.* **27**, 148 (1990).

47. M. E. Field and K. A. Kvenvolden, *Geology* **13**, 517 (1985); J. M. Brooks, M. E. Field, M. C. Kennicutt II, *Mar. Geol.* **96**, 103 (1991); P. G. Brewer *et al.*, *Eos* **78**, 340 (1997)

48. P. Lonsdale, *AAPG Bull.* **69**, 1160 (1985).

49. We thank personnel of the Ocean Drilling Program for their efforts during drilling and assistance with sampling. We also thank D. Krause for encouragement and enlightening discussions during this work and for review of the manuscript. Critical inspiration came from the work of E. Nisbet and G. Dickens. We thank two anonymous reviewers for constructive advice. Careful technical assistance was provided by K. Thompson and H. Berg. Supported by NSF grant EAR99-0424 (Earth System History) and an NSF Fellowship to I.L.H. Twenty-five percent of this research was funded by the National Institute for Global Environmental Change through the U.S. Department of Energy (DOE) (Cooperative Agreement DE-FC03-90ER61010). Conclusions expressed in this publication are those of the authors and do not necessarily reflect the views of the DOE.

18 October 1999; accepted 23 February 2000

Sink or Swim: Strategies for Cost-Efficient Diving by Marine Mammals

Terrie M. Williams,[1]* R. W. Davis,[2] L. A. Fuiman,[3] J. Francis,[4] B. J. Le Boeuf,[1] M. Horning,[2] J. Calambokidis,[5] D. A. Croll[6]

Locomotor activity by diving marine mammals is accomplished while breath-holding and often exceeds predicted aerobic capacities. Video sequences of freely diving seals and whales wearing submersible cameras reveal a behavioral strategy that improves energetic efficiency in these animals. Prolonged gliding (greater than 78% descent duration) occurred during dives exceeding 80 meters in depth. Gliding was attributed to buoyancy changes with lung compression at depth. By modifying locomotor patterns to take advantage of these physical changes, Weddell seals realized a 9.2 to 59.6% reduction in diving energetic costs. This energy-conserving strategy allows marine mammals to increase aerobic dive duration and achieve remarkable depths despite limited oxygen availability when submerged.

Swimming is energetically expensive for mammals and results in transport costs that are 2 to 23 times the levels predicted for fish (*1, 2*). To reduce these costs, marine mammals have de-

[1]Department of Biology, EMS-A316, University of California, Santa Cruz, CA 95064, USA. [2]Department of Marine Biology, Texas A&M University, 5007 Avenue U, Galveston, TX 77553, USA. [3]Department of Marine Science, University of Texas at Austin, 750 Channel View Drive, Port Aransas, TX 78373, USA. [4]Committee for Research and Exploration, National Geographic Society, 1145 17th Street NW, Washington, DC 20036, USA. [5]Cascadia Research, 218½ West Fourth Avenue, Olympia, WA 98501, USA. [6]Institute of Marine Science, EMS-A316, University of California, Santa Cruz, CA 95064, USA.

*To whom correspondence should be addressed. E-mail: williams@darwin.ucsc.edu

veloped a wide variety of energy-conserving swimming behaviors. Adherence to a narrow range of routine transit speeds (*3, 4*), wave-riding (*5*), and porpoising (*6*) decrease the amount of energy expended when pinnipeds and cetaceans move near the water surface. Although these energy-conserving strategies are especially beneficial during underwater activity, when access to ambient oxygen is limited, two of the behaviors, porpoising and wave-riding, cannot be used when the animal is submerged. In view of this, it has been assumed that marine mammals swim constantly at cost-efficient routine speeds during diving (*3, 4*). Indeed, the routine speeds of many freely diving marine mammals fall within a relatively narrow range (*7, 8*). A paradox arises when

metabolic rates are assigned to these swimming speeds. Calculations based on measured speeds during diving and metabolic rates for bottlenose dolphins swimming near the water surface predict that the animals would be unable to complete a 200-m-deep dive using aerobic metabolic pathways. Yet, dolphins perform these dives with only small changes in postdive plasma lactate concentrations, where elevated levels would indicate a transition to anaerobic metabolism (9). Similar discrepancies between predicted aerobic capabilities and diving performance have been reported for a wide variety of marine birds and mammals (10, 11). The mechanisms by which these divers resolve the apparent conflict between the energetic demands of swimming and the conservation of limited oxygen stores during submergence are not understood (12, 13). Metabolic depression (14) and regional heterothermy (15) associated with cardiovascular changes during diving have been suggested, although the influence of activity level has not been assessed. This has been due in part to the difficulty of observing and monitoring diving animals at depth.

Here, we monitored locomotor behavior during diving with video cameras carried by free-ranging cetaceans and pinnipeds. Unlike other instruments placed on marine mammals in which behavior has been inferred from time-depth records or velocity profiles (16), video images permit direct observation of swimming periods, stroke frequency, and glide sequences. Coupled with time-depth recorders, these new tools allowed us to assess the locomotor strategies used by marine mammals throughout their dives.

Subjects for this study included three adult Weddell seals (*Leptonychotes weddellii*, body mass = 393 ± 2 kg) diving from an isolated ice hole in McMurdo Sound, Antarctica (17), a juvenile northern elephant seal (*Mirounga angustirostris*, 263 kg) freely diving in Monterey Bay, California (17), an adult bottlenose dolphin (*Tursiops truncatus*, 177 kg) trained to dive to submerged targets offshore of San Diego, California (18), and an adult blue whale (*Balaenoptera musculus*, estimated mass = 100 tons) traveling offshore of northern California along Cordell Bank (19). Each animal carried a submersible video system with a camera facing either forward to record movements of the head or backward to record propulsive movements of the flukes or hind flippers. Data loggers simultaneously monitored duration and depth of dives.

Instrumented animals were free to perform sequential dives in open water or, in the case of the Weddell seals, below the frozen sea ice. The video system and instrumentation were retrieved when the animals hauled out (Weddell seals, elephant seal) or returned to a trainer (dolphin), or the package was detached by a release mechanism (blue whale). Swimming mode, relative stroke am-

plitude, stroke frequency, and gliding periods were determined for each video sequence, using a motion analysis system (Peak Performance, Englewood, Colorado). These data were then matched to duration and depth of the associated dive (20). To assess the effect of changes in locomotor pattern on energetic costs, we measured postdive oxygen consumption of instrumented Weddell seals breathing into a metabolic hood (21, 22).

Despite independent evolution of swimming in cetaceans and pinnipeds, and differences in body size and propulsive mechanisms, we found a similar sequence of locomotor gaits during diving for the four species examined (Fig. 1). Diving descents began with 30 to 200 s of continuous stroking that was followed by a marked, prolonged period of gliding to maximum depth. Gliding began at similar depths (86 ± 10 m, n = 3 species) and continued to the bottom of the dive for the seals and dolphin, although maximum dive depths ranged from 115 to 385 m. The blue whale began gliding at comparatively shallower depths (18 ± 1 m, n = 3 dives) during dives of 36 to 88 m in depth. Descent rate during the glide varied little among the three smaller species (1.1 ± 0.1 m s^{-1}, n = 3 species), whereas the blue whale descended considerably slower at 0.3 to 0.4 m s^{-1}. The absolute duration of stroking or gliding sequences depended on maximum depth and dive duration. Deep divers (the phocid seals) showed the longest absolute glide periods. Maximum glide duration was 6.0 min for the juvenile elephant seal descending to nearly

400 m and 6.2 min for an adult Weddell seal descending to 540 m.

Initial ascent of each dive was characterized by sequential, large-amplitude strokes. The range of frequencies during steady stroking on initial ascent was 60 to 110 strokes min^{-1} (1.0 to 1.8 Hz) for the three smaller species (dolphin, elephant seal, Weddell seal). In comparison, the range of stroke frequencies was one-tenth of this range (6 to 10 strokes min^{-1}; 0.1 to 0.2 Hz) for the massive blue whale. Ascent rate during the period of constant stroking was 1.0 ± 0.2 m s^{-1} for all four species examined.

Following the period of continuous stroking, the animals switched to stroke-and-glide swimming for the remainder of the ascent except for a short (<100 s) glide to the surface. Only the Weddell seals did not glide the final 10 m to the surface, a behavior that was undoubtedly influenced by the presence of the sea ice and the maneuvering required to reach the isolated ice hole.

The similarity in locomotor behaviors for these four species is striking given the ranges of body sizes and propulsive mechanisms. Both cetaceans use dorsoventral undulations of a lunate tail for propulsion (23). The two pinniped species swim with alternate lateral sweeps of paired hind flippers in which the posterior half of the body may flex (24).

Passive gliding by the seals and dolphin began at nearly identical depths, suggesting that changes in hydrostatic pressure and buoyant forces prompted the incorporation of prolonged glide sequences during descent. Previous stud-
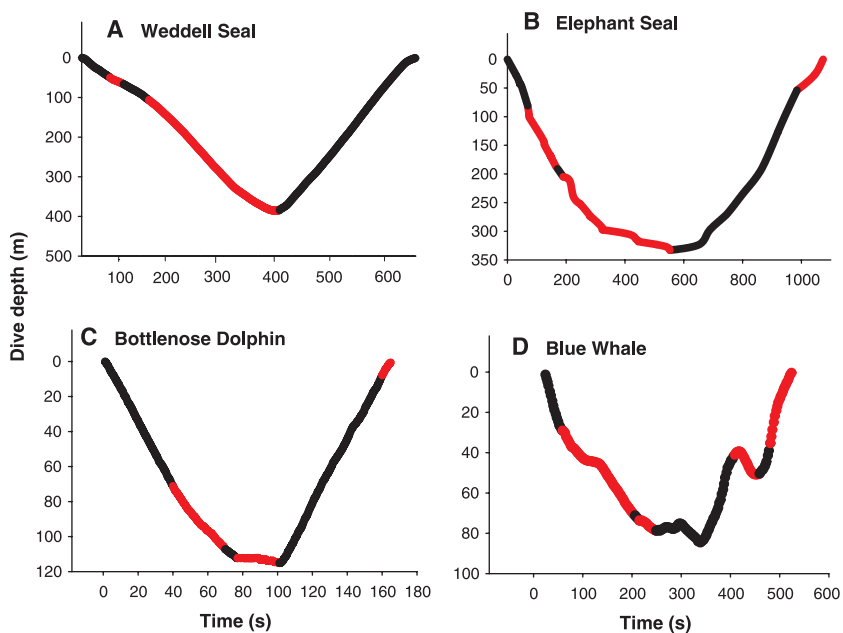

Fig. 1. Locomotor activity of four species of diving marine mammal. Representative deep dives are presented for the (**A**) Weddell seal (maximum depth = 385 m), (**B**) northern elephant seal (333 m), (**C**) bottlenose dolphin (115 m), and (**D**) blue whale (84 m). Each curve represents dive depth in relation to time elapsed during the dive. Color of the line corresponds to stroking (black) and gliding (red) periods. Stroking periods include both continuous stroking and stroke-and-glide activities. Note the prolonged gliding period during descent for each species.

ies have shown that bottlenose dolphins (*25*) and elephant seals (*26*) modify ascent and descent rates during deep dives in response to changes in buoyancy. In dolphins diving to 100 m, the magnitude of the buoyant force changes from positive (+24.3 N) near the water surface to negative (–25.7 N) at depths exceeding 67 m (*25*). These changes are attributed to the gradual collapse of the lungs and a decrease in lung volume that occur with increasing hydrostatic pressure during descent. Complete collapse of the alveoli occurs once dolphins have reached pressures equivalent to 65 to 70 m in depth (*27, 28*). Likewise, the morphological structure of the respiratory system of elephant seals and Weddell seals indicates the capacity for collapse that may affect buoyancy during the course of a dive (*29, 30*). Because compression of the air spaces decreases the volume of the animal without a change in mass, buoyancy decreases on descent. When the downward force of negative buoyancy exceeds drag forces, the animal may glide passively during descent, thereby avoiding the energetic costs associated with active stroking.

As might be expected, dive depth, and therefore distance traveled, affects the percentage of time available for gliding. The percentage of time spent gliding during descent increased significantly ($n = 53$, $r^2 = 0.70$, $P < 0.001$) and nonlinearly with increasing dive depth (Fig. 2). This percentage ranged from 10 to 63% for shallow dives of less than 100 m and reached a plateau of 82 ± 2% ($n = 21$) for deep dives exceeding 200 m. All deep dives were by the phocid seals. Blue whales also showed extended gliding sequences that exceeded 78% of the descent period for dives to 88 m.

A reduction in locomotor effort afforded by gliding should be manifested as a decrease in energetic cost. This has been reported for short-duration glides associated with intermittent (stroke-and-glide) locomotion in fish (*31*) and diving birds (*32, 33*). We found a similar result for Weddell seals that incorporated prolonged glides during diving (Fig. 3). Oxygen consumption during the recovery periods of individual dives was measured for three adult, free-ranging seals wearing video instrumentation (*21, 22*). Two groups of dives covering similar distances but differing in gliding and swimming behaviors were compared (*34*). Dives incorporating gliding during descent resulted in a 9.2 to 59.6% (mean = 27.8 ± 5.5%, $n = 10$) reduction in recovery oxygen consumption compared with dives using stroke-and-glide or continuous swimming. In general, greater savings occurred with deep dives, which is consistent with the increase in the proportion of time gliding with depth (Fig. 2). In view of these results, there appears to be a significant energetic advantage to gliding rather than swimming on descent by marine mammals.

The value of the energetic savings is demonstrated by examining the effect on the oxygen reserves of the diving seal. A 400-kg Weddell seal stores 87 ml of O_2 per kg of body weight (ml O_2 kg^{-1}) in its lungs, blood and muscle to support aerobic metabolism while submerged (*10, 11*). An average energetic savings of 27.8% (Fig. 3) due to prolonged gliding represents 24.2 ml O_2 kg^{-1}. The metabolic rate of Weddell seals during rest or low levels of underwater activity was 3.2 ml O_2 kg^{-1} min^{-1}. At this metabolic rate, the oxygen saved by gliding allows the seal to extend its aerobic dive time by 7.5 min (24.2 ml O_2 kg^{-1} divided by 3.2 ml O_2 kg^{-1} min^{-1}) assuming the same level of activity. This additional time represents 38% of the routine 20-min dive duration of free-ranging Weddell seals. The energetic savings could make the difference between completing a dive aerobically or relying on anaerobic metabolism with the coincident disadvantages associated with the accumulation of lactate and prolonged recovery (*10, 11*). For marine mammals that are hunting, these savings may increase the overall efficiency of foraging. During traveling, the energetic savings when submerged may reduce the cost of long-distance migrations.

The ability of marine mammals to take advantage of physical changes at depth permits the conservation of limited oxygen stores during submergence. These results provide insight into the means by which diving marine mammals resolve the conflict between the energetic demands of swimming and the need for energy conservation during submergence. Prolonged gliding behavior by diving marine mammals appears to be a general phenomenon, irrespective of the method of propulsion and size of the animal. Even the largest mammalian diver, the blue whale, displays this behavior.

Fig. 2. Percentage glide time during descent in relation to dive depth for four species of marine mammal. Each point represents an individual dive. The data were described by the nonlinear function, percentage glide time =

$$85.9 - \left(\frac{2820.3}{\text{Depth}}\right)$$

($n = 53$, $r^2 = 0.70$, $P < 0.001$). Except for the dolphins, the range of depths was determined by the free-ranging behavior of the instrumented animals.
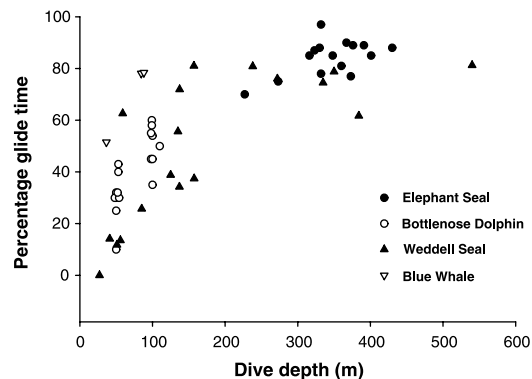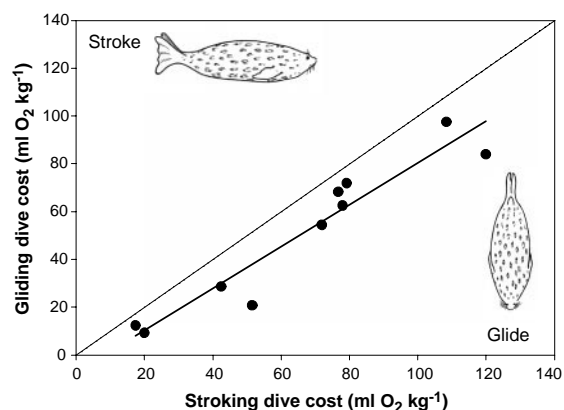

Fig. 3. Recovery oxygen consumption of gliding dives in relation to stroking dives for free-ranging Weddell seals (*34*). Each point represents a gliding dive paired with a stroking dive of equal distance traveled (±60 m) for an individual seal. Total distance traveled ranged from 354 to 3614 m, which resulted in the range of energetic costs. The thin line through the origin represents the line of equality for the cost of gliding dives and stroking dives. The thick solid line denotes the least-squares linear regression through the data points. Dives incorporating prolonged gliding were consistently less costly than stroking dives of similar distance, as described by glide cost = 0.88 stroke cost – 7.30 ($n = 10$, $r^2 = 0.91$, $P < 0.001$). Consequently, all paired dives fell below the line of equality.

References and Notes

1. K. Schmidt-Nielsen, *Science* **177**, 222 (1972).
2. T. M. Williams, *Philos. Trans. R. Soc. London Ser. B* **354**, 193 (1999).
3. D. Thompson, A. R. Hiby, M. A. Fedak, *Symp. Zool. Soc. London* **66**, 349 (1993).
4. T. M. Williams, W. A. Friedl, J. E. Haun, N. K. Chun, *Symp. Zool. Soc. London* **66**, 383 (1993).
5. T. M. Williams *et al.*, *Nature* **355**, 821 (1992).
6. D. Au and D. Weihs, *Nature* **284**, 548 (1980).
7. P. J. Ponganis *et al.*, *Can. J. Zool.* **68**, 2105 (1990).
8. P. M. Webb, thesis, University of California at Santa Cruz (1999).
9. T. M. Williams, J. E. Haun, W. A. Friedl, *J. Exp. Biol.* **202**, 2739 (1999).
10. G. L. Kooyman and P. J. Ponganis, *Annu. Rev. Physiol.* **60**, 19 (1998).
11. P. J. Butler and D. R. Jones, *Physiol. Rev.* **77**, 837 (1997).
12. M. A. Castellini *et al.*, *J. Appl. Physiol.* **58**, 392 (1985).
13. P. W. Hochachka, *FASEB Fed. Proc.* **45**, 2948 (1986).
14. _____, *Experientia* **48**, 570 (1992).
15. Y. Hadrich *et al.*, *Nature* **388**, 64 (1997).
16. D. E. Crocker, B. J. Le Boeuf, D. P. Costa, *Can. J. Zool.* **75**, 27 (1997).
17. The experimental setup and instrumentation for Weddell seals are described in (*35*). Similar instrumentation was deployed on an elephant seal captured at Año

Nuevo Point, CA, and released offshore in Monterey Bay. After release, the seals returned to instrumentation sites where the data and videos were retrieved.

18. The experimental setup and instrumentation for the dolphin studies are described in (25). The instrument pack was neutrally buoyant and weighed 8 kg in air. Twenty experimental dives from 50 to 110 m were conducted in open water.

19. Blue whale studies used CRITTERCAM instrumentation (36) attached with a low-profile silicon suction cup (22 cm diameter). The cup released after a predetermined interval through the dissolution of a corrosible magnesium plug. The blue whale (length = 22 to 25 m) had been individually identified photographically during 1990–98 along the California coast. It was considered an adult of at least 10 years in age.

20. Gliding was defined as periods exceeding 3 to 12 s in which no locomotor movements occurred and flippers or flukes were aligned along the body axis. Deployments involving forward-facing cameras on Weddell seals also used a tail-mounted ±2-g, single-axis accelerometer (Ultramarine Instruments, Galveston, TX) to assess stroking activity. Head movements of the blue whale were considered indicative of stroke activity because of counter movements of the head and tail in swimming cetaceans (25, 37). Videotapes were reviewed at normal speed, except for the blue whale;

cycling rate was increased sevenfold to facilitate analyses of the exceptionally slow movements of the whale.

21. R. W. Davis, T. M. Williams, G. L. Kooyman, Physiol. Zool. 58, 590 (1985).

22. M. A. Castellini, G. L. Kooyman, P. J. Ponganis, J. Exp. Biol. 165, 181 (1992).

23. F. E. Fish, J. Exp. Biol. 201, 2867 (1998).

24. ———, S. Innes, K. Ronald, J. Exp. Biol. 137, 157 (1988).

25. R. C. Skrovan, T. M. Williams, P. S. Berry, P. W. Moore, R. W. Davis, J. Exp. Biol. 202, 2749 (1999).

26. P. M. Webb, D. E. Crocker, S. B. Blackwell, D. P. Costa, B. J. Le Boeuf, J. Exp. Biol. 201, 2349 (1998).

27. S. H. Ridgway, B. L. Scronce, J. Kanwisher, Science 166, 1651 (1969).

28. S. H. Ridgway and R. Howard, Science 206, 1182 (1979).

29. G. L. Kooyman, D. D. Hammond, J. P. Scholander, Science 169, 82 (1970).

30. Because seals exhale before diving, the relative contribution of lung compression to changes in buoyancy during diving is unknown for pinnipeds. The large, incompressible blubber layer of pinnipeds is less dense than seawater and may represent a significant component of the upward buoyant force (26).

31. D. Weihs, J. Theor. Biol. 48, 215 (1974).

32. R. Stephenson, J. Exp. Biol. 190, 155 (1994).

33. J. R. Lovvorn, D. A. Croll, G. A. Liggins, J. Exp. Biol. 202, 1741 (1999).

34. Stroking dives, as determined from accelerometer data, were characterized by the absence of prolonged (>10 s) gliding periods and stroke-and-glide or continuous flipper movements. Gliding dives incorporated prolonged periods of gliding that ranged from 10.7 to 52.2% (mean = 36.0 ± 4.8%, n = 9; 58 to 803 s) of total dive duration.

35. R. W. Davis et al., Science 283, 993 (1999).

36. G. Marshall, Mar. Technol. Soc. J. 32, 11 (1998).

37. J. J. Videler and P. Kamermans, J. Exp. Biol. 119, 265 (1985).

38. Supported by Office of Naval Research (ONR) grant N00014-95-1-1023 and NSF Polar Programs grant OPP-9618384 to T.M.W., and ONR grant N00014-99-1-0192 to D.A.C. Blue whale research was supported through National Geographic Television. We thank G. Marshall for development of CRITTERCAM used in the blue whale study and W. Hagey for instrumentation used in the seal and dolphin studies. We also thank E. Roscow and T. Tinker for assistance with the illustrations. Animal studies were approved by individual institutional Animal Use Committees using NIH guidelines.

29 December 1999; accepted 8 March 2000

Identification of a Coordinate Regulator of Interleukins 4, 13, and 5 by Cross-Species Sequence Comparisons

G. G. Loots,[1,2] R. M. Locksley,[3] C. M. Blankespoor,[1] Z. E. Wang,[3] W. Miller,[4] E. M. Rubin,[1]* K. A. Frazer[1]*

Long-range regulatory elements are difficult to discover experimentally; however, they tend to be conserved among mammals, suggesting that cross-species sequence comparisons should identify them. To search for regulatory sequences, we examined about 1 megabase of orthologous human and mouse sequences for conserved noncoding elements with greater than or equal to 70% identity over at least 100 base pairs. Ninety noncoding sequences meeting these criteria were discovered, and the analysis of 15 of these elements found that about 70% were conserved across mammals. Characterization of the largest element in yeast artificial chromosome transgenic mice revealed it to be a coordinate regulator of three genes, interleukin-4, interleukin-13, and interleukin-5, spread over 120 kilobases.

Computational methods for recognizing coding sequences in genomic DNA are capable of detecting most genes; however, identifying regulatory elements in the 95% of the genome composed of noncoding sequences is currently a substantial challenge. Regulatory sequences tend to be highly conserved among mammals (1), suggesting comparative sequence analysis as a strategy for their identification (2). Extensive studies focusing on understanding the regulation of three biomedically important cytokines [interleukin-4 (IL-4), IL-13, and IL-5] clustered at human 5q31 have indicated that these genes are coordinately coactivated in type 2 T helper (T$_H$2) cells (3). Transgenic mice propagating human 5q31 yeast artificial chromosomes (YACs) appropriately regulate the human IL-4, IL-13, and IL-5 transgenes in murine T$_H$2 cells, independent of the site of integration (4). These data indicate that the elements regulating the coordinate tissue and temporal expression of these cytokines are con-

served in humans and mice. A comparative sequence-based approach was employed to discover distant regulatory sequences involved in controlling the complex expression patterns of the 5q31 cytokines.

Database searches combined with GenScan predictions identified 23 putative genes (including IL-4, IL-13, and IL-5) in an ~1-Mb human 5q31 region and determined that the order and orientation of all but one of these genes are conserved in the murine chromosome 11 orthologous region (Fig. 1) (5–7). Comparative analysis of these human and mouse sequences (8) focused on discovering distant regulatory sequences in the region, based on the observation that these elements are typically composed of long sequences [≥100 base pairs (bp) in length] that are highly conserved among mammals (≥70% identity) (1). A total of 245 conserved elements fitting these criteria was identified, of which 155 overlapped with coding sequences (defined as sequences present in mature RNA transcripts) (9), and the remaining 90 were defined as noncoding (Figs. 1 and 2) (10). Of the 90 conserved noncoding elements, 46% were in introns, 9% were within 1 kb of the 5′ and 3′ ends of an identified transcript, and 45% were in intergenic regions >1 kb from any known gene. Many of the noncoding elements were found in clusters, such as in the intergenic region between organic cation transporter 1 (OCTN1) and P4–hydroxylase alpha (II), suggesting that they may be working cooperatively as a functional unit (Fig. 1). One of the conserved noncoding sequences (CNSs), CNS-7, located in the intergenic region between granulocyte-macrophage colony-stimulating factor (GM-CSF) and IL-3, had previously been identified experimentally as an enhancer controlling the coregulation of these two cytokines (11). This finding supports the choice of the criteria used in this sequence-based approach to iden-

[1]Genome Sciences Department, Lawrence Berkeley National Laboratory, Berkeley, CA 94720, USA. [2]Department of Molecular and Cell Biology, University of California, Berkeley, CA 94720, USA. [3]Departments of Medicine and Microbiology/Immunology and Howard Hughes Medical Institute, University of California, San Francisco, CA 94143, USA. [4]Department of Computer Science and Engineering, Pennsylvania State University, University Park, PA 16802, USA.

*To whom correspondence should be addressed. E-mail: kafrazer@lbl.gov (K.A.F.) and emrubin@lbl.gov (E.M.R.)